# Composite Band-Gap Solitons in Nonlinear Optically Induced Lattices

Anton S. Desyatnikov,[1,2] Elena A. Ostrovskaya,[2] Yuri S. Kivshar,[2] and Cornelia Denz[1]

[1]*Nonlinear Photonics Group, Institute of Applied Physics, Westfälische Wilhelms-Universität Münster, D-48149 Münster, Germany*

[2]*Nonlinear Physics Group and Centre for Ultra-high Bandwidth Devices for Optical Systems (CUDOS), Research School of Physical Sciences and Engineering, Australian National University, Canberra ACT 0200, Australia*

(Received 8 April 2003; published 8 October 2003)

We introduce novel optical solitons that consist of a periodic and a spatially localized component coupled nonlinearly via cross-phase modulation. The spatially localized optical field can be treated as a gap soliton supported by the optically induced nonlinear grating. We find different types of these band-gap composite solitons and demonstrate their dynamical stability.

DOI: 10.1103/PhysRevLett.91.153902 PACS numbers: 42.65.Tg

Recent theoretical and experimental results demonstrated nonlinear localization of light in optically induced refractive-index gratings [1,2]. Such localized states can be treated as "discrete" and "gap" solitons observed in fabricated periodic photonic structures [3], but supported by gratings induced by a complementary optical field. Optically induced lattices open up an exciting possibility for creating dynamically reconfigurable photonic structures in bulk nonlinear media. The physics of coherent light propagating in periodic gratings can be linked to the phenomena exhibited by coherent matter waves (Bose-Einstein condensates) in optical lattices [4].

Among the most challenging problems in the physics of induced gratings is the creation of stable, uniform periodic optical patterns which can effectively modulate the refractive index of a nonlinear medium. Periodic modulation of the refractive index can be induced, for instance, by an interference pattern illuminating a photorefractive crystal with a strong electro-optic anisotropy [1]. Interfering plane waves modulate the space-charge field in the crystal, which relates to the refractive index via electro-optic coefficients. The latter are substantially different for the two orthogonal polarizations. As a result, the material nonlinearity experienced by waves polarized in the direction of the $c$ axis of the crystal is up to 2 orders of magnitude larger than that experienced by the orthogonally polarized ones. When the lattice-forming waves are polarized orthogonally to the $c$ axis, the nonlinear self-action as well as any cross action from the copropagating probe beam can be neglected. The periodic interference pattern propagates in the diffraction-free linear regime, thus creating a stationary refractive-index grating [2].

In this Letter we develop the concept of optically induced gratings beyond the limit of weak material nonlinearity and propose the idea of robust nonlinearity-assisted optical lattices, created by nonlinear periodic waves. Strong incoherent interaction of such a grating with a probe beam, through the nonlinear cross-phase-modulation (XPM) effect, facilitates the formation of a novel type of a composite optical soliton, where one of the components creates a periodic photonic structure, while the other component experiences Bragg reflection from this structure and can form gap solitons localized in the transmission gaps of the linear spectrum. The observation of nonlinear light localization in this type of optically induced gratings can be achieved in photorefractive medium with two incoherently interacting beams of the same polarization. Effectively incoherent interaction of these beams can be achieved by exploiting the slow nonlinear response of a photorefractive crystal [5]. We study such a configuration in a saturable medium and demonstrate the existence and stable dynamics of the novel band-gap lattice solitons.

The propagation of two incoherently interacting beams in a photorefractive crystal can be approximately described by the coupled nonlinear Schrödinger (NLS) equations for the slowly varying envelopes $E_n$ ($n = 1, 2$),

$$i\frac{\partial E_n}{\partial z} + \frac{\partial^2 E_n}{\partial x^2} + \sigma N(I) E_n = 0, \tag{1}$$

where $N(I) = I/(1 + sI)$ describes saturable nonlinearity, $I = \sum |E_n|^2$ is the total light intensity, $s$ is the saturation parameter, and $\sigma = \pm 1$ stands for the focusing or defocusing nonlinearity, respectively. Stationary solutions are found in the form $E_n = u_n(x)\exp(i\sigma k_n z)$, where $k_n$ are the propagation constants of the components. We assume strong saturation regime, $s = 1$, which is closer to realistic experimental conditions.

The induced waveguiding regime, well studied in the context of vector solitons [3], corresponds to the case when the intensities of the two interacting fields are significantly different. Then the strong field (e.g., $u_1$) is described by a single (scalar) NLS equation, and the weaker field propagates in the effective linear waveguide induced by the stronger component via XPM. Here we assume that the effective waveguide (i.e., the grating) is created by a periodic nonlinear field $u_1(x)$ with the propagation constant $k_1$, described by the stationary wave-train solutions of a scalar Eq. (1) (see also Ref. [6]). Integrating the stationary form of Eq. (1) once, we introduce the effective potential $P(u_1) = (\sigma/2)[(1 - k_1)u_1^2 - \ln(1 + u_1^2)]$, so that

  

the general stationary solution $u_1(x)$ with the amplitude $A$ can be found by solving the equation $P(A) = \frac{1}{2}(du_1/dx)^2 + P(u_1)$. Figure 1(a) shows the form of the potential $P(u_1)$ in both the focusing ($\sigma = +1$, top) and the defocusing ($\sigma = -1$, bottom) cases. The minima of $P(u_1)$ correspond to a plane wave with the constant amplitude $A_{\rm cw}^2 = k_1/(1 - k_1)$, whereas the bright soliton solutions correspond to the separatrix at $A = A_s$ with $P(A_s) = 0$.

In the limit $s \to 0$, exact analytical expressions for the nonlinear periodic waves $u_1(x)$ can be written down for $\sigma = \pm 1$, in terms of the elliptic Jacobi functions, $\mathrm{cn}(x, \mu)$, $\mathrm{dn}(x, \mu)$, and $\mathrm{sn}(x, \mu)$, with the modulus $0 \leq \mu(k_1) \leq 1$. They represent self-consistent solutions of the cubic NLS equations which coincide with the well-studied Hill equation with associated Lamé potentials [7]. It can be shown that the general structure of the periodic solutions is preserved for $s \neq 0$. For $\sigma = +1$, there exist two branches of the periodic (cnoidal) solutions shown through their induced refractive-index modulation in Fig. 1(d) for $A = A_1$, $A_{\rm cw} < A_1 < A_s$, and in Fig. 1(e) for $A = A_2 > A_s$. The cn-type solutions of the branch $A_2$ have nodes, whereas the dn-type solutions of the branch $A_1$ are nodeless. In the defocusing case ($\sigma = -1$), there exists only one branch of the sn-type periodic solutions for $A = A_0 < A_{\rm cw}$; see Fig. 1(c). In a strongly nonlinear limit the large-period $A_{1,2}$ and $A_0$ solutions describe periodic trains of bright and dark solitons, respectively.

Having identified the stationary structure of nonlinear periodic waves $u_1(x)$, we find that, in the induced waveguiding regime, the weak probe $u_2$ is scattered by an effectively fixed linear grating characterized by the potential $N(I)$, where $I = u_1^2(x)$. The guiding properties of such a linear grating are determined by the band-gap structure of the spectrum of the Hill equation: $d^2u_2/dx^2 = -\sigma N(I)u_2 + k_2 u_2$, where the eigenvalue $k_2(A)$ depends on the grating amplitude. The eigenfunctions satisfy the Bloch condition $u_2(x) = \exp(iKL)u_2(x + L)$, where $L$ is the period and $K$ is the momentum of the lattice. The spectrum consists of $M$ bands and a continuum band, with the total $m = 2M + 1$ band edges. The eigenfunction at the $m$th band edge corresponds to a strictly periodic Bloch wave $u_2^m \equiv b^m(x) = \pm b^m(x + L)$, for which $KL = 0, \pi$. Figure 2 shows an example of the band-gap spectrum $-k_2$ generated by the scalar cnoidal wave $u_1(x)$, for $k_1 = 0.5$. The Bloch waves at the band edges $m = 1, 2, 3, 4, 5, \ldots$ have the propagation constants $-\sigma k_2^m \leq -\sigma k_2^{m+1}$ and the periods $L, 2L, 2L, L, L, \ldots$. The Bloch wave $b^m(x)$ at the band edge $k_2^m = k_1$ coincides with the scalar cnoidal wave $u_1(x)$. In the case of a saturable nonlinearity some predictions of the number and position of the bands and gaps can be made using the theory of Lamé-type equations [8]. For example, in the case of a defocusing nonlinearity, the grating potential can be well approximated by $N(x) \approx a(a + 1)\mu \mathrm{sn}^2(x, \mu)$, where $a = 1$. Since the spectrum of the Lamé equation has $M = a$ bound bands, it is expected that the $A_0$-type grating generates a single bound band followed by a semi-infinite band (as seen in Fig. 2 for $A < A_{\rm cw}$).

In the limit $A \to A_s$ the period of the cnoidal-wave solution diverges and the spectrum bands disappear. On the other hand, when the grating amplitude $A$ approaches the plane-wave amplitude $A_{\rm cw}$ in the focusing case, the periodic modulation of the refractive index vanishes and the gaps disappear; see Fig. 2.

To be useful for creation of robust dynamical photonic structures, nonlinear periodic waves should be stable. Previous studies of stability of periodic solutions [6,9,10] suggest that the solutions of the $A_1$-type are strongly unstable due to modulational instability (MI), whereas MI is suppressed for the $A_2$-type solutions in a saturable medium, and also for $A_0$-type solutions in the defocusing case. Our numerical studies have confirmed that the $A_0$-type grating in the defocusing case is both linearly and dynamically stable, and also demonstrated

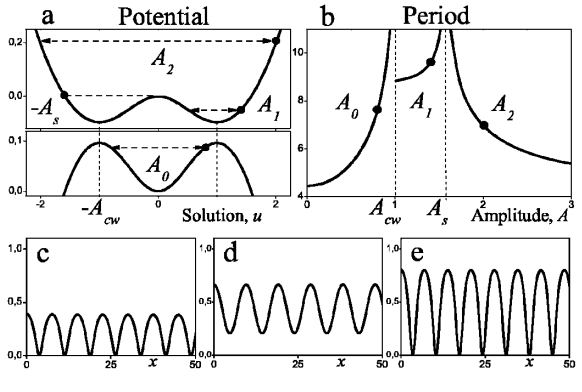


FIG. 1. (a) Effective potential $P(u_1)$ for the focusing (top) and defocusing (bottom) cases ($k_1 = 0.5$). Period (b) and examples (c)–(e) of the refractive-index modulation $N(I)$ for the three branches of periodic solutions of the NLS equation: (c) $A_0 = 0.8$, (d) $A_1 = 1.41$, and (e) $A_2 = 2.01$.

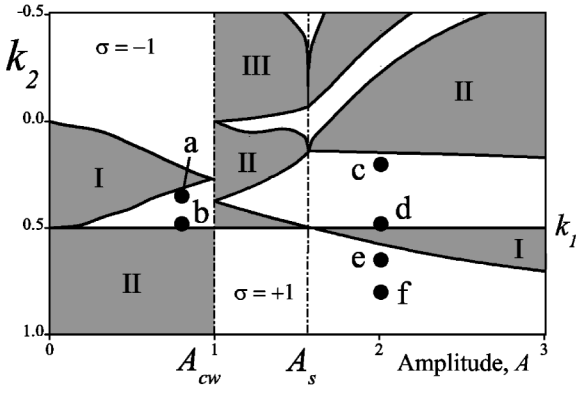


FIG. 2. The band-gap structure of the linear spectrum $-k_2(A)$, induced by the nonlinear periodic grating $u_1(x)$ for $k_1 = 0.5$. The bands are shaded. Marked dots indicate the propagation constants for gap solitons shown in Fig. 3.

that the $A_2$-type solutions are only weakly (oscillatory) unstable. In contrast, the $A_1$-type lattice is quickly destroyed by strong symmetry-breaking instabilities; therefore, we excluded it from our further consideration.

The localization of the probe field $u_2$ in the gaps of the linear spectrum of the periodic structure induced by the field $u_1(x)$ can occur in the nonlinear regime of the probe propagation. In this regime, the significant intensity of the probe beam causes its nonlinear self-action. When the backaction of the probe on the grating through XPM is ignored (e.g., in the case of a weak material nonlinearity for the grating wave), the physics of the localization is similar to the standard case of nonlinear waves in fixed periodic potentials, well studied in the context of both optical and matter waves [4,9,11,12]. However, in our problem the grating and scattered wave are strongly nonlinearly coupled and, therefore, as in the case of two-component vector solitons [3], we should expect the existence of self-consistent hybrid structures formed by a periodic wave and a localized gap mode.

Indeed, by solving two-component Eq. (1) numerically, with a value of $k_1$ fixed to that of the scalar grating $k_1 = k_1^g$, we have found different families of solutions, consisting of the oscillatory ($u_1$) and localized ($u_2$) mutually trapped constituents. The propagation constant of the localized component always lies within the gaps of the linear spectrum. Therefore this component can be described as a gap soliton with even or odd symmetry [12], centered at a maximum or minimum of the grating potential, respectively. Figure 3 shows some examples of such a gap soliton for both defocusing and focusing cases. In Fig. 4 we show different families of the localized modes. First, we note that the powers of discrete solitons with different symmetries coincide, i.e., these solitons belong to the same family. This indicates the absence of the Peierls-Nabarro potential barrier and good mobility of the localized states. Second, due to the nonlinear XPM interaction, the induced grating is strongly modified by the localized component, but recovers periodicity in the far field.

In agreement with the theory of gap solitons [12], the families of localized states originate at the edges of the bands with the numbers $m = 2$ (for $\sigma < 0$) or $m = 1, 3, 5, \ldots$ (for $\sigma > 0$), where the effective dispersion, $(\partial^2 k_2/\partial K^2)|_{k_2^m}$, is correspondingly negative or positive. At the respective band edge, the low-power gap soliton is weakly localized, and can be described as a slowly varying envelope of the corresponding Bloch wave $b^m(x)$ [11]. In the defocusing case, only gap solitons [(a) and (b) in Figs. 2–4] can exist in the induced grating, whereas in the focusing case, both gap [(c) and (d)] solitons and self-trapped [(e) and (f)] solitons in the semi-infinite gap are possible. Near the opposite gap edges, where the gap modes have high powers, the periodic grating wave acquires significant defects induced by the localized state; however, both components still form a vector stationary state.

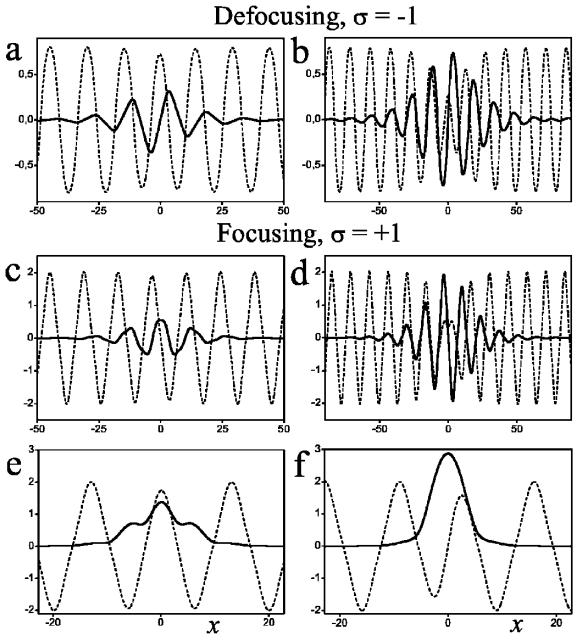


FIG. 3. Examples of the stationary two-component solutions in the different band gaps for fixed parameters of the periodical component $k_1 = 0.5$ for the defocusing medium (upper row) and the focusing medium (two lower rows). The dashed lines are the periodic component $u_1$; the solid lines are the localized component $u_2$. Gap solitons correspond to the marked points in Fig. 4.

To understand the nature of this composite state, we consider the correction to the linear grating spectrum due to the low-amplitude gap mode $u_2$, which is bifurcating off the lower edge of band II ($m = 3$) in the focusing case, or upper edge of band I ($m = 2$) in the defocusing case. Near the bifurcation threshold, the nonlinear XPM coupling leads to the effective shift of the propagation constant of the periodic grating component: $k_1 = k_1^g + \Delta k_1$,

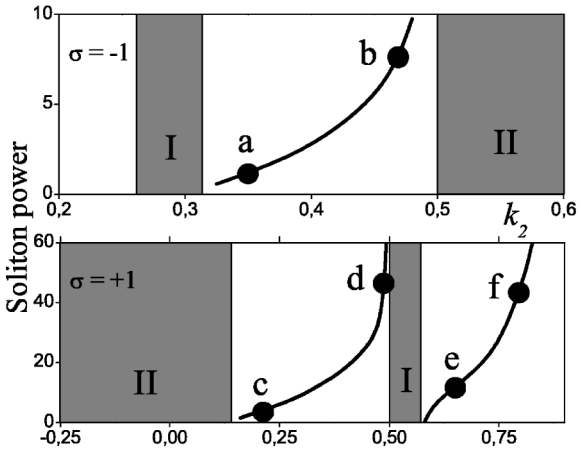


FIG. 4. Power of the localized component $Q = \int u_2^2(x)dx$ vs $k_2$ for $k_1 = 0.5$ and defocusing ($A_0 = 0.8$) (top) and focusing ($A_2 = 2.01$) (bottom) nonlinearity. Shaded regions correspond to the spectral bands, and the solid circles mark the solutions shown in Fig. 3.

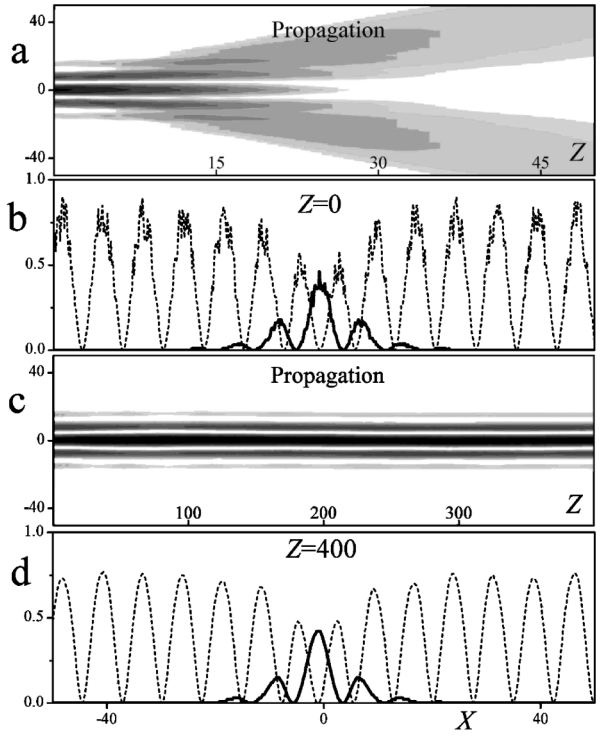


FIG. 5. Stable propagation of the gap soliton in the defocusing grating. (a) Propagation dynamics of the initial (odd) state, corresponding to the family (a) and (b) in Fig. 4, perturbed by a random amplitude noise, in the absence of the grating; (b) the gap mode (solid line) and grating (dashed line) initial profiles; (c) propagation dynamics in the presence of the grating; (d) the final state at $z = 400$.

where $k_1^g$ is the fixed propagation constant for the scalar grating $u_1^g(x)$, and $\Delta k_1 \sim \sigma \int u_2^2 u_1^2 (1 + u_1^2)^{-2} dx$. As a result, the band edges $k_2^m$ corresponding to the periodic Bloch modes $b^m(x) = u_1^g(x)$ shift into the gap. This means that the nonlinear mode $u_1$, coupled to the field $u_2$ and corresponding to the fixed propagation constant $k_1 = k_1^g$ (i.e., fixed power), now lies within the band, and has an oscillatory, but not strictly periodic, nature. Therefore, the localized low-power gap mode $u_2$ is nonlinearly coupled to an in-band defect mode in the $u_1$ component, which is localized on the Bloch-wave background. Together, the two components form a novel band-gap composite soliton. In the deeply nonlinear regime, when the high-intensity gap mode induces a large defect in the grating wave, both components exist as a vector soliton in a periodic waveguide $N(I)$, which depends on both field intensities, $I = u_1^2 + u_2^2$. As $k_2 \to k_1$, the gap mode's amplitude approaches that of the grating, and both components of the band-gap soliton become oscillatory.

The crucial issue of stability of the gap solitons in the nonlinear induced gratings is therefore linked to the stability of the composite band-gap states. We have confirmed dynamical stability of band-gap solitons by numerical integration of the vector dynamical model (1). Figure 5 shows an example of the stationary propagation of an odd gap soliton [family (a) and (b) in Fig. 4] in an induced nonlinear grating for the defocusing case. Both components are initially perturbed by a random noise at 20% of their peak amplitude [Fig. 5(b)]. If the grating is removed, the localized gap mode can no longer be supported by the defocusing nonlinearity and strongly diffracts [Fig. 5(a)]. Being coupled to the lattice, the gap mode generates a defect in the grating and coexists with it as a dynamically stable composite state, which is clearly robust to perturbations [Figs. 5(c) and 5(d)].

In conclusion, we have introduced novel composite band-gap solitons where one of the components creates a periodic nonlinear lattice which localizes the other component in the form of a gap soliton. Nonlinear localization of this kind should be generic to models of nonlinearly interacting multicomponent fields, where one of the components can exist in a dynamically stable self-modulated periodic state. Here, we considered a specific example of a spatial nonlinear photonic structure induced by optical beams in a photorefractive crystal. Another example is the dynamical Bragg gratings for optical pulses obtained through the cross-phase modulation in highly birefringent fibers [13].

The authors appreciate the critical reading of the manuscript by A. A. Sukhorukov and gratefully acknowledges support of the Humboldt Foundation and the Australian Research Council.

[1] N. K. Efremidis *et al.*, Phys. Rev. E **66**, 046602 (2002).
[2] J. W. Fleischer *et al.*, Phys. Rev. Lett. **90**, 023902 (2003); Nature (London) **422**, 147 (2003); D. Neshev *et al.*, Opt. Lett. **28**, 710 (2003).
[3] Yu. S. Kivshar and G. P. Agrawal, *Optical Solitons: From Fibers to Photonic Crystals* (Academic, San Diego, 2003), p. 560.
[4] P. J. Louis *et al.*, Phys. Rev. A **67**, 013602 (2003); E. A. Ostrovskaya and Yu. S. Kivshar, Phys. Rev. Lett. **90**, 160407 (2003).
[5] G. I. Stegeman and M. Segev, Science **286**, 1518 (1999).
[6] V. A. Aleshkevich, V. A. Vysloukh, and Ya. V. Kartashov, Quantum Electron. **31**, 257 (2001).
[7] V. M. Petnikova, V. V. Shuvalov, and V. A. Vysloukh, Phys. Rev. E **60**, 1009 (1999); A. Khare and U. Sukhatme, J Math Phys (N.Y.) **40**, 5473 (1999).
[8] E. T. Whittaker and G. N. Watson, *A Course of Modern Analysis* (Cambridge University Press, Cambridge, 1980).
[9] J. C. Bronski *et al.*, Phys. Rev. Lett. **86**, 1402 (2001).
[10] S. E. Fil'chenkov, G. M. Fraiman, and A. D. Yunakovskii, Sov. J. Plasma Phys. **13**, 554 (1987).
[11] J. E. Sipe and H. G. Winful, Opt. Lett. **13**, 132 (1988).
[12] A. A. Sukhorukov and Yu. S. Kivshar, Phys. Rev. E **65**, 036609 (2002).
[13] S. Pitois, M. Haelterman, and G. Millot, Opt. Lett. **26**, 780 (2001).